Biochimica et Biophysica Acta 1818 (2012) 3090–3097

Contents lists available at SciVerse ScienceDirect

Biochimica et Biophysica Acta

journal homepage: www.elsevier.com/locate/bbamem

Oligomeric state study of prokaryotic rhomboid proteases

Padmapriya Sampathkumar, Michelle W. Mak, Sarah J. Fischer-Witholt, Emmanuel Guigard, Cyril M. Kay, M. Joanne Lemieux *,[1]

Department of Biochemistry, University of Alberta, Edmonton, Alberta, Canada T6G 2H7

ARTICLE INFO

Article history:
Received 18 June 2012
Received in revised form 25 July 2012
Accepted 7 August 2012
Available online 18 August 2012

Keywords:
GlpG
Rhomboid protease
Rhomboid peptidase
Intramembrane protease
Oligomerization
Dimerization

ABSTRACT

Rhomboid peptidases (proteases) play key roles in signaling events at the membrane bilayer. Understanding the regulation of rhomboid function is crucial for insight into its mechanism of action. Here we examine the oligomeric state of three different rhomboid proteases. We subjected *Haemophilus influenzae*, (*hi*GlpG), *Escherichia coli* GlpG (*ec*GlpG) and *Bacillus subtilis* (YqgP) to sedimentation equilibrium analysis in detergent-solubilized dodecylmaltoside (DDM) solution. For *hi*GlpG and *ec*GlpG, rhomboids consisting of the core 6 transmembrane domains without and with soluble domains respectively, and YqgP, predicted to have 7 transmembrane domains with larger soluble domains at the termini, the predominant species was dimeric with low amounts of monomer and tetramers observed. To examine the effect of the membrane domain alone on oligomeric state of rhomboid, *hi*GlpG, the simplest form from the rhomboid class of intramembrane proteases representing the canonical rhomboid core of six transmembrane domains, was studied further. Using gel filtration and crosslinking we demonstrate that *hi*GlpG is dimeric and functional in DDM detergent solution. More importantly co-immunoprecipitation studies demonstrate that the dimer is present in the lipid bilayer suggesting a physiological dimer. Overall these results indicate that rhomboids form oligomers which are facilitated by the membrane domain. For *hi*GlpG we have shown that these oligomers exist in the lipid bilayer. This is the first detailed oligomeric state characterization of the rhomboid family of peptidases.

1. Introduction

Rhomboid proteases belong to the family of S54 intramembrane serine proteases (peptidases) [1]. Identified in all kingdoms of life with the exception of viruses [2,3], they play diverse functions in signaling. As intramembrane proteases, they carry out proteolysis of transmembrane substrates within or proximal to the lipid bilayer. The cleavage event releases a peptide signal that can in turn play a role in various cellular events. For review see [4].

Rhomboid proteases represent significant targets of study owing to their essential biological roles and their involvement in human disease. In *Drosophila*, where rhomboids were discovered, rhomboids are critical for cell fate [5]. Rhomboid dysfunction or overexpression plays vital roles in the pathologies of cancer and other important human diseases. In humans, elevated levels of the Golgi associated rhomboid family-1 protein (RHBDF-1) and rhomboid domain containing 2 protein, (RHBDD2) have been identified in breast cancer [6–8]. RHBDD2 has been shown to cleave epidermal growth factor (EGF) resulting in EGF receptor activation [9], a receptor known to play a role in several cancers [10]. The mitochondrial form of rhomboid, presenilin-associated rhomboid-like (PARL), is known to participate in mitochondrial membrane fusion, an essential function for the maintenance of mitochondria dynamics and apoptosis [11,12]. PARL has been shown to play roles in Parkinson's disease [13] and autosomal dominant optic atrophy [14]. In addition to cancer and Parkinson's disease, rhomboids are involved with the establishment of malarial infection. Invasion by malarial parasite *Plasmodium* relies on the function of ROM1, a rhomboid protease [15].

The function of a few rhomboid peptidases has also been examined in prokaryotes. In the pathogenic *Providencia stuartii* rhomboids have been shown to cleave the TatA protein which forms the TatA translocon, affecting quorum sensing [16–18]. Understanding how prokaryotic extracellular factors affect intracellular signaling may allow us to further understand the effect of quorum sensing on virulence and biofilm formation [19]. YqgP (also known as GluP) has been shown to play a role in cell division and glucose uptake in *Bacillus subtilis* [20]. Mutational studies with GlpG from *Escherichia coli*

Abbreviations: AU, analytical ultracentrifugation; DDM, n-dodecyl-β-D-maltopyranoside or dodecylmaltoside; GF, gel filtration; *hi*GlpG, *Haemophilius influenzae* GlpG; *ec*GlpG, *Escherichia coli* GlpG

* Corresponding author. Tel.: +1 780 492 3586; fax: +1 780 492 0886.
E-mail address: joanne.lemieux@ualberta.ca (M.J. Lemieux).
[1] Canada Research Chair and AIHS Scholar.

0005-2736/$ – see front matter © 2012 Elsevier B.V. All rights reserved.
http://dx.doi.org/10.1016/j.bbamem.2012.08.004

(*ec*GlpG) revealed no significant phenotype except an increase in resistance to cefotaxime, a β-lactam antibiotic [21]. The biological function of *ec*GlpG remains undetermined.

Insight into the function of rhomboid proteases has been gained from several crystal structures. Rhomboid proteases have a core of six transmembrane helices observed in the crystal structures of *hi*GlpG [22] and the membrane domain structure of *ec*GlpG [23–26]. Other topologies are predicted with an extra transmembrane helix at the N-terminus or C-terminus. Some rhomboid families have large N-terminal cytoplasmic domains or large soluble domains found between helices 1 and 2. Approximately 10 Å below the extracellular membrane surface is the active site catalytic dyad consisting of residues Ser and His. These residues are conserved in all functional rhomboids [27,28]. While this is unique from the traditional Asp-His-Ser catalytic triad, several examples do exist of serine proteases having catalytic dyads [29]. Co-crystallization with a coumarin and phosphonofluoridate inhibitors has given insight into substrate cleavage within the membrane demonstrating the involvement of these conserved residues [30–32]. The buried active site led to questions regarding how substrates gain access. The inhibitor structures along with mutagenesis with *ec*GlpG and a recent crystal structure with *hi*GlpG have demonstrated that a flexible helix acts as a substrate gate allowing access to the buried active site [31,33,34].

Little is known about the regulation of rhomboid protease function. Rhomboids from various species are functional in the membrane as well as in detergent solubilized solution [28,35]. Interestingly, reconstitution with different lipids can influence the activity of the peptidase [35]. Although the functions of various rhomboid enzymes have been examined, little biophysical characterization has been carried out on this family of peptidases.

During our initial attempts to crystallize rhomboid proteases, we identified that they formed oligomers. This led us to investigate their oligomeric state since membrane proteins often function as oligomers as a means of regulating their function [36–38]. In this paper, we demonstrate that the rhomboid with the six-TMD core *hi*GlpG, *ec*GlpG behave as dimers in detergent solution while YqgP having 7 TMDs and a large cytoplasmic domain behaves as tetramers. The 6 TMD core was analyzed further using the *hi*GlpG rhomboid peptidase which, using both crosslinking and gel filtration, behaved as a dimer both in detergent solution and co-immunoprecipitation experiments from membrane suggesting that rhomboids behave as dimers in the lipid bilayer.

2. Experimental procedures

2.1. Cloning and expression

*ec*GlpG was generated using PCR with an *E. coli* strain DH5α, while YqgP and *hi*GlpG were generated by PCR using genomic *B. subtilis* and *Haemophilus influenzae* DNA, respectively, and purchased from ATCC, USA. Using restriction digestion, PCR products were then ligated into pBAD-MycHisA vector (Invitrogen, Canada).

2.1.1. Membrane fraction isolation

E. coli (Top10) expressing *ec*GlpG, *hi*GlpG, and YqgP were grown to an $OD_{600} = 1.0$, 0.4 and 1.0, respectively and induced with 0.0002% arabinose at 24 °C for 5 h. Cells were harvested at 7000 rpm (12,227 *g*) for 10 min using an Avanti J1.8000 rotor (Beckman, USA). Cells were resuspended in 4 volumes TBS supplemented with and EDTA-free peptidase inhibitor cocktail (NEB, USA) 1 mM PMSF, 0.1 mg/ml DNase, and lysed using an EmulsiFlex-C3, (Avestin Inc., Ottawa, Canada). Unbroken cells were pelleted in a JA17 rotor at 15,000 rpm (10,000 *g*) for 20 min. Membrane fractions were collected by ultracentrifugation in an L8-80 ultracentrifuge at 35,000 rpm (100,000 *g*) in a 45Ti rotor (Beckman, USA).

2.1.2. Protein purification

Membrane fractions were homogenized in 50 mM Tris, 300 mM NaCl, 30 mM imidazole, 20% glycerol, and 1% DDM pH 8.0. The solution was stirred for 30 min followed by ultracentrifugation for 30 min at 45,000 rpm (110,000 *g*) in a 45Ti rotor (Beckman, USA). The supernatant was incubated with Ni-NTA resin (Qiagen, Ontario, Canada) for 2 h. The resin was then collected and washed with 20 column volumes (CV) of 50 mM Tris, 300 mM NaCl, 30 mM imidazole, 20% glycerol, and 0.1% DDM pH 8.0 followed by 20 CV of the above stated buffer with 35 mM imidazole. Protein fractions were eluted in a step-wise manner with 3× 2 CV of the above described buffer containing 250, 500 and 1000 mM imidazole. Bicinchoninic acid (BCA) kit (Pierce Biotechnology Inc., Thermo Scientific, Il, USA) was used to determine protein concentrations. The proteins were finally purified using gel filtration as described below and then subjected to SDS-PAGE.

2.2. Analytical ultracentrifugation

Sedimentation equilibrium experiments were conducted at 20 °C in a Beckman XL-I analytical ultracentrifuge using absorbance optics, as described by Laue and Stafford [39]. Protein samples used for DDM runs were obtained after Ni-NTA. Prior to runs, samples were dialyzed for at least 48 h in 20 mM Tris, 20 mM NaCl pH 8.0 and 0.05% DDM. Aliquots (110 μl, 1 mg/ml) of the sample solution were loaded into six sector CFE sample cells, allowing three concentrations to be run simultaneously. Runs were performed at a minimum of three different speeds and each speed was maintained until there was no significant difference in $r^2/2$ versus absorbance scans taken 2 h apart to ensure that equilibrium had been achieved. Sedimentation equilibrium data were evaluated using the NONLIN program, which employs a nonlinear least squares curve-fitting algorithm described by Johnson et al. [40]. The program allows analysis of both single and multiple data files and can be fit to models containing up to four associating species, depending upon which parameters are permitted to vary during the fitting routine. The protein's partial specific volume and the solvent density were estimated using the Sednterp program [41]. DDM amounts were quantified using thin layer chromatography.

2.2.1. Thin layer chromatography detection of DDM

A 20 μl sample of *hi*GlpG was obtained post Ni-NTA purification containing 9.2 μg of protein, along with DDM standards was spotted directly onto silica glass plates (Whatman, USA). The mobile solvent phase consisted of ethylacetate/methanol 4:1 (v/v). The plate was sprayed with 2 N H_2SO_4 solution and then charred at 90 °C for DDM detection [42].

2.3. Detergent solubilized hiGlpG crosslinking

Crosslinking of *hi*GlpG was studied using dithiobis (succinimidylpropionate), (DSP; Pierce Protein Research Products, Thermo Fisher Scientific, Rockford, USA) and 3,3′-dithiobis (sulfosuccinimidylpropionate), (DTSSP; Pierce Protein Research Products, Thermo Fisher Scientific, Rockford, USA). For each crosslinker, three aliquots of 10 μg (20 μl) of *hi*GlpG- post-Ni-NTA purification were dialyzed with PBS (pH 7.4). One aliquot was treated as the control. The remaining two aliquots were incubated with either 1 mM DSP or 1 mM DTSSP respectively, for 30 min at room temperature. Reactions were quenched with 1 M Tris, pH 7.5 to a final concentration of 50 mM. To one of the crosslinked aliquots, 1 M DTT was added to a final concentration of 50 mM and incubated at 37 °C for 30 min. All samples were then subjected to SDS-PAGE under non-reducing conditions and transferred to Hybond-P PVDF membrane (GE Healthcare, USA). Western blots were probed with His probe — HRP (Santa Cruz Biotechnology) at 1:500 dilution and followed by rabbit anti-mouse antibody conjugated to horseradish

peroxidase at 1:40,000 dilution. Bands were detected using ECL Plus western blot detection system (GE Healthcare, USA).

2.4. Activity assay

Providencia stuartii TatA (*ps*TatA) was supplied as a gift from Dr. Matthew Freeman, MRC, Cambridge in a pET21a vector. PCR was used to introduce a Flag-tag at the N-terminus. *ps*TatA-Flag protein was used for the functional assay and purified as previously described for the C100-TatA construct [33]. *hi*GlpG was purified with 0.1% DDM as above except tags were removed using a 1 h digestion with 30 U thrombin per mg of protein followed by flash freezing in liquid nitrogen. 15 μg rhomboid was added to 500 ng of *ps*TatA substrate along with DDM to a final concentration of 0.1% in a 20 μl reaction volume. The reaction was incubated at 37 °C for 1 h and stopped with SDS-PAGE buffer. Samples were resolved on (4%/16%) SDS-PAGE and transferred to Hybond-P PVDF membranes (GE Healthcare, USA). Western blots were probed with mouse anti-Flag antibody at 1:10,000 dilution followed by an anti-mouse antibody conjugated to HRP (1:80,000 dilution). Signal was detected with ECL Plus western blotting detection reagents (GE Healthcare, USA).

2.5. Gel filtration chromatography

*hi*GlpG obtained from a Ni-NTA purification as described above, was subjected to thrombin digestion (9 units of thrombin/mg *hi*GlpG) overnight at room temperature. Approximately 200 μg of the digested sample was injected onto a Hiload Superdex 200 10/300 column (GE Healthcare, USA) equilibrated with 50 mM Tris, 200 mM NaCl, 5% glycerol, pH 8.0 and 0.1% DDM. Samples were run at 0.3 ml/min flow rate and monitored at 280 nm absorbance. V_0 is the column void volume, and V_t is the column total volume accessible to solvent [43]. The standard proteins used were thyroglobulin (MW, 670 k; Stokes radius 85 Å), IgG (MW 158, Stokes radius 55 Å), ovalbumin; (MW 44 k; Stokes radius 30.5 Å), myoglobin (MW 17 k, Stokes radius 20.7 Å). The standard curve was constructed using the molecular weights of standard proteins versus their *Ve/Vo* values, from which the mass of the eluted protein samples were calculated.

2.6. Anti-Flag-pull down assay

2.6.1. Plasmid constructs

His-tagged and Flag-tagged *hi*GlpG were constructed individually by Quikchange mutagenesis (Stratagene, CA) by using pBAD-*hi*GlpG-myc.His as the template. Mutations were verified by DNA sequencing. The PCR products were cut by NcoI/HindIII and cloned into NcoI/HindIII digested pACYCDuet1 and pET28a (Novagen, USA) to generate pACYCDuet1-*hi*GlpG-His_6 and pET28a-*hi*GlpG-Flag respectively.

2.6.2. Protein expression and purification

E. coli BL21/DE3 cells harboring pACYCDuet1-*hi*GlpG-His, pET28a-*hi*GlpG-Flag or both were grown at 37 °C in LB medium supplemented with appropriate antibiotics [ampicillin (100 μg/ml) for pACYCDuet1-*hi*GlpG-His, kanamycin (30 μg/ml) for pET28a-*hi*GlpG-Flag or both (for co-transformed plasmids)]. Transformants were grown to an OD_{600} of 0.8 and induced with 0.1 mM IPTG for 6 h. Cells were harvested at 7000 rpm (12,227 *g*) for 15 min using Avanti JLA8.1000 rotor and then were resuspended in 4 volumes of TBS supplemented with EDTA-free protease inhibitor cocktail (Roche, USA), 0.1 mg/ml DNase and disrupted using an EmulsiFlex-C3 (Avestin Inc, Ottawa, Canada). Unbroken cells and cell debris were pelleted in a JA17 rotor at 15,000 rpm (10,000 *g*) for 20 min. Membrane fractions were collected by ultracentrifugation at 35,000 rpm (100,000 *g*) for 2 h at 4 °C in a 45Ti rotor (Beckman, USA).

Membrane pellets were then homogenized with 50 mM Tris (pH 8.0), 300 mM NaCl, 10 mM imidazole, 20% glycerol and protease inhibitor tablets. Membrane homogenates of *hi*GlpG-His, *hi*GlpG-Flag, and coexpressed (*hi*GlpG-His and *hi*GlpG-Flag) were aliquoted (1 ml) and solubilized with 1% DDM for 30 min at 4 °C followed by ultracentrifugation at 40,000 rpm (100,000 *g*) for 30 min at 4 °C in a TLS 55 rotor (Beckman, USA). For the mixed-membrane control, 0.5 ml of *hi*GlpG-His membrane fraction was mixed with 0.5 ml of *hi*GlpG-Flag membrane fraction after homogenization on ice for 30 min and solubilized as above.

Aliquots of supernatant of each of above fractions (1 ml) were incubated with 50 μl of pre-equilibrated Flag affinity resin (Anti-Flag M2 Affinity Gel; Sigma, USA) for 2 h at 4 °C with agitation for protein binding. Resins were washed with 20 column volumes of TBS supplemented with 0.1% DDM. Immunocomplexes were finally dissolved in SDS sample buffer and analyzed by Western blotting. To ensure that equal amounts of the protein was added to the resin an SDS-PAGE gel (4%/12%) was prepared simultaneously and stained with Coomassie blue R250.

2.6.3. Western blotting

Equal amounts of the immunocomplexes were loaded onto separate 4%/12% SDS-PAGE gels and proteins were electroblotted to Hybond-P PVDF membrane (GE Healthcare, USA) at 100 V for 1 h. Membranes were blocked with 3% skim milk in TBST and probed with His probe-HRP (Santa Cruz Biotechnology) at 1:1000 dilution (for *hi*GlpG-His proteins) or anti-Flag antibody (Sigma, USA) at 1:10,000 dilution (for *hi*GlpG-Flag proteins) followed by a rabbit anti-mouse antibody conjugated to horseradish peroxidase at 1:80,000 dilution. Bands were detected using ECL Plus western blot detection system (GE Healthcare, USA).

3. Results

3.1. Overexpression

Three prokaryotic rhomboid orthologs, *hi*GlpG from *H. influenzae*, *ec*GlpG from *E. coli*, and YqgP from *B. subtilis*, were analyzed for protein overexpression. Final cell culture parameters for all rhomboids resulted in the use of 0.002% arabinose with a 5 h induction time at 24 °C. Protein purification for all rhomboids was carried out in dodecylamaltoside (DDM, Anatrace, USA) using Ni-NTA column purification as previously described for *hi*GlpG [44]. Expression yields post-purification using the His-tag affinity Ni-NTA resin were as follows: 1.8 mg/l for *hi*GlpG, 2.0 mg/l *ec*GlpG, and 1.6 mg/l for YqgP. All proteins were subjected to gel filtration chromatography for further purification, resulting in a single band on SDS-PAGE (Fig. 1).

3.2. Oligomeric state of three prokaryotic rhomboid peptidases

In order to assess the oligomeric state of the three rhomboid peptidases, *hi*GlpG, *ec*GlpG and YqgP were purified in DDM and subjected to sedimentation equilibrium analysis by analytical ultracentrifugation (Table 1 and Fig. 2). All speeds for each sample, *hi*GlpG, *ec*GlpG, and YqgP, are also shown (Supplementary Figs. 2, 3, 4). A global mass of 135,079 Da, 141,476 Da and 203,989 Da was obtained for *hi*GlpG, *ec*GlpG and YqgP respectively. Thin layer chromatography was used to assess detergent amounts associated with *hi*GlpG, 45 K ± 5 (Supp. Fig. 1) [45]. This is in agreement with the amount of radiolabelled DDM associated with a membrane protein LacS that consists of 12 transmembrane segments, which was calculated to be 100 K of DDM per monomer [46]. When the global mass obtained from the sedimentation equilibrium is divided by the mass of the rhomboid peptidases plus the detergent bound, we get two rhomboid molecules per species for *hi*GlpG, ecGlpG and YqgP (Table 1), indicating that these prokaryotic rhomboids preferentially form a dimer in detergent solution. The best-fit analysis is in agreement with all proteins fitting to a monomer–dimer–tetramer model with a dimer being the predominant species for *hi*GlpG and *ec*GlpG. Best fit analysis with YqgP indicated that more tetramers were observed compared to *hi*GlpG and *ec*GlpG.

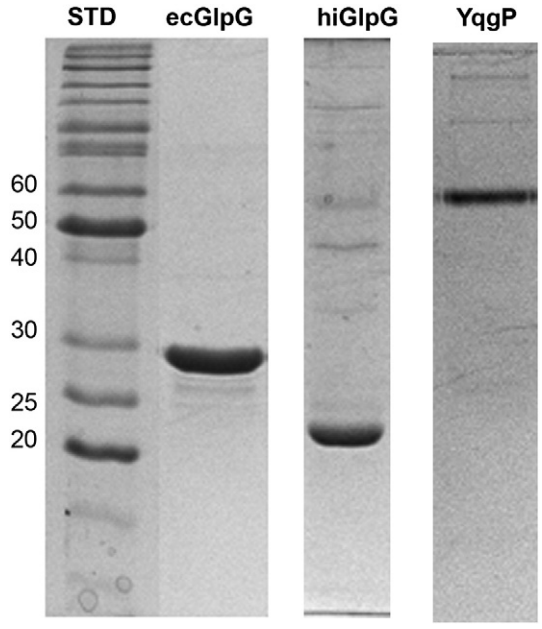

Fig. 1. Overexpression of prokaryotic rhomboid peptidases. SDS-PAGE of overexpressed prokaryotic rhomboid peptidases: *ec*GlpG from *Escherichia coli*, *hi*GlpG from *Haemophilus influenzae*, and YqgP (GluP) from *Bacillus subtilis*.

To further analyze the oligomeric state of rhomboids and determine whether the membrane domain is responsible for the dimerization, we focused solely on the *hi*GlpG. Sequence analysis indicates that this is the simplest form of the rhomboid family of proteins [47]. Its crystal structure indeed confirms it having only 6 transmembrane segments with no large N- or C-terminal domains [44].

3.3. Crosslinking studies with detergent solubilized hiGlpG indicate a dimeric species

We analyzed the oligomeric state of DDM solubilized *hi*GlpG using the homobifunctional crosslinking reagents, DTSSP and DSP. These are membrane impermeant and membrane permable reagents, both of which react covalently with amino groups, and their internal disulfide bond can be cleaved by reducing reagents such as DTT. These two crosslinkers were initially chosen to distinguish between crosslinking with loop and transmembrane segments. The molecular weight of the *hi*GlpG-MycHis is 25,061 Da, however when resolved on SDS-PAGE, the protein runs at 23 kDa (Fig. 1). When crosslinked samples were resolved on SDS-PAGE and blotted on a PVDF membrane for Western blot analysis, we could see that both DSP and DTSSP efficiently cross-linked *hi*GlpG and the dimeric species could be seen at 45 kDa, the expected molecular weight for a dimer (Fig. 3). Followed by the addition of DTT, a reducing agent that separates the homobifunctional crosslinkers, the cross-linked products were cleaved and found to be migrating at the same molecular weight as that of the monomer. Slightly more crosslinking is observed with the membrane permeant DSP compared to the impermeant DTSSP. Two of the three lysines in *hi*GlpG are located at the base of transmembrane segments and DSP being membrane permeant may be able to penetrate the detergent micelle more readily compared to DTSSP. We do not observe 100% crosslinking which is typical for membrane proteins. A weak dimer band is observed in the control lane without crosslinker suggesting a strong interaction between dimers that is not fully separated by SDS. In addition we see a faint band in the crosslinking samples at approximately 70 K near the trimer range, however the absence of a trimer in the gel filtration (see below) and analytical ultracentrifugation experiments suggests this may be a minor contaminant crosslinking with *hi*GlpG.

Table 1
Summary of sedimentation equilibrium results shown is the calculated G1pG mass post thrombin cleavage, without detergent, calculated molecular weight (MW) obtained from adding the protein mass with the calculated amount detergent of detergent bound (39,843 Da, see Supplementary information), the global fit MW. The ratio to calculate the quaternary state was obtained by dividing the global fit MW by the protein plus detergent molecular weight. Bold indicates predominant species found during the analysis.

Protein in DDM	Protein (Da)	Protein + Det. MW	Global fit M.W.	Best fit	Monomer/global best fit
*hi*GlpG	22,124	61,967	135,079	M–**D**–T	2.3
*ec*GlpG	31,772	71,615	141,476	M–**D**–T	2.0
YqgP	54,700	94,543	203,989	M–T	2.2

3.4. Gel filtration of hiGlpG rhomboid peptidase reveals that the functional species is dimeric

To determine if the dimer was indeed the predominant species for *hi*GlpG, Ni-NTA purified sample was run on an analytical gel filtration (GF) column (Fig. 4A). Examination of the profile for *hi*GlpG reveals retention time of the eluted *hi*GlpG just below the 158 kDa marker. Given approximately 45 K of detergent (approximately one micelle of DDM) associated with one *hi*GlpG (Supplementary Fig. 1) suggests we have a dimer under these conditions. In support of this data, preparative gel filtration carried out on *hi*GlpG in DDM using a Superdex200 (16/60) column results in an elution time identical to that observed for GlpT transporter which has twelve transmembrane segments and is monomeric in DDM [48] (data not shown). In addition we also observe a shoulder peak approximately half of the height of the major peak eluting at 12 ml retention time. Using the standard curves, regression analysis calculation for the molecular weight for this peak indicates a mass of approximately 265 kDa suggesting that a tetrameric species is also present which is in agreement with the analytical centrifugation results.

In order to assess if the dimer was active, Ni-NTA purified *hi*GlpG was also subjected to a gel-based activity assay, typical for intramembrane proteases [33,35] (Fig. 4b). *P. stuartii* TatA (*ps*TatA) with an N-terminal Flag tag was used as the substrate. In the presence of *hi*GlpG, psTatA was cleaved that was assessed by Western blotting using anti-Flag antibody, indicating that the dimeric *hi*GlpG is functional.

3.5. Co-purification of hiGlpG-His and hiGlpG-Flag shows rhomboid forms dimers in the membrane bilayer

To test if *hi*GlpG formed dimers within the membrane, we designed a co-expression study to allow the expression of two different *hi*GlpGs: one with a His tag and the other with a Flag tag. DDM-solubilized membranes were isolated from cells co-expressing *hi*GlpG-His and *hi*GlpG-Flag. DDM-solubilized membranes were also isolated from cells expressing each individual clone of *hi*GlpG-His and *hi*GlpG-Flag to serve as controls. As a negative control, individual membranes of *hi*GlpG-His and *hi*GlpG-Flag were mixed prior to the addition of detergent to ensure that dimers did not form as a result of the solubilization step. Anti-Flag affinity gel was used to purify the proteins and the presence of dimers in the immunoprecipitated fractions was examined by Western blotting with either anti-Flag antibody or His-Probe. Fractions expressing Flag tagged proteins that immunoprecipitated with Flag affinity resin were detected by the anti-Flag antibody (Fig. 5A). As expected, *hi*GlpG-His was not detected by Anti-Flag antibody. The blot was also subsequently probed with the His-Probe (Fig. 5B). In the co-expressed fraction purified with Flag resin, *hi*GlpG-His was detected demonstrating that the two epitopes were found to coimmunoprecipitate. This indicates that *hi*GlpG-Flag and *hi*GlpG-His associate within the membrane. In order to rule out the possibility that the co-immunoprecipitation was due to the disruption of the dimers, a control was included where the His- and Flag-tagged dimers was expressed and purified independently. The separately purified proteins were then subjected to the same detergent

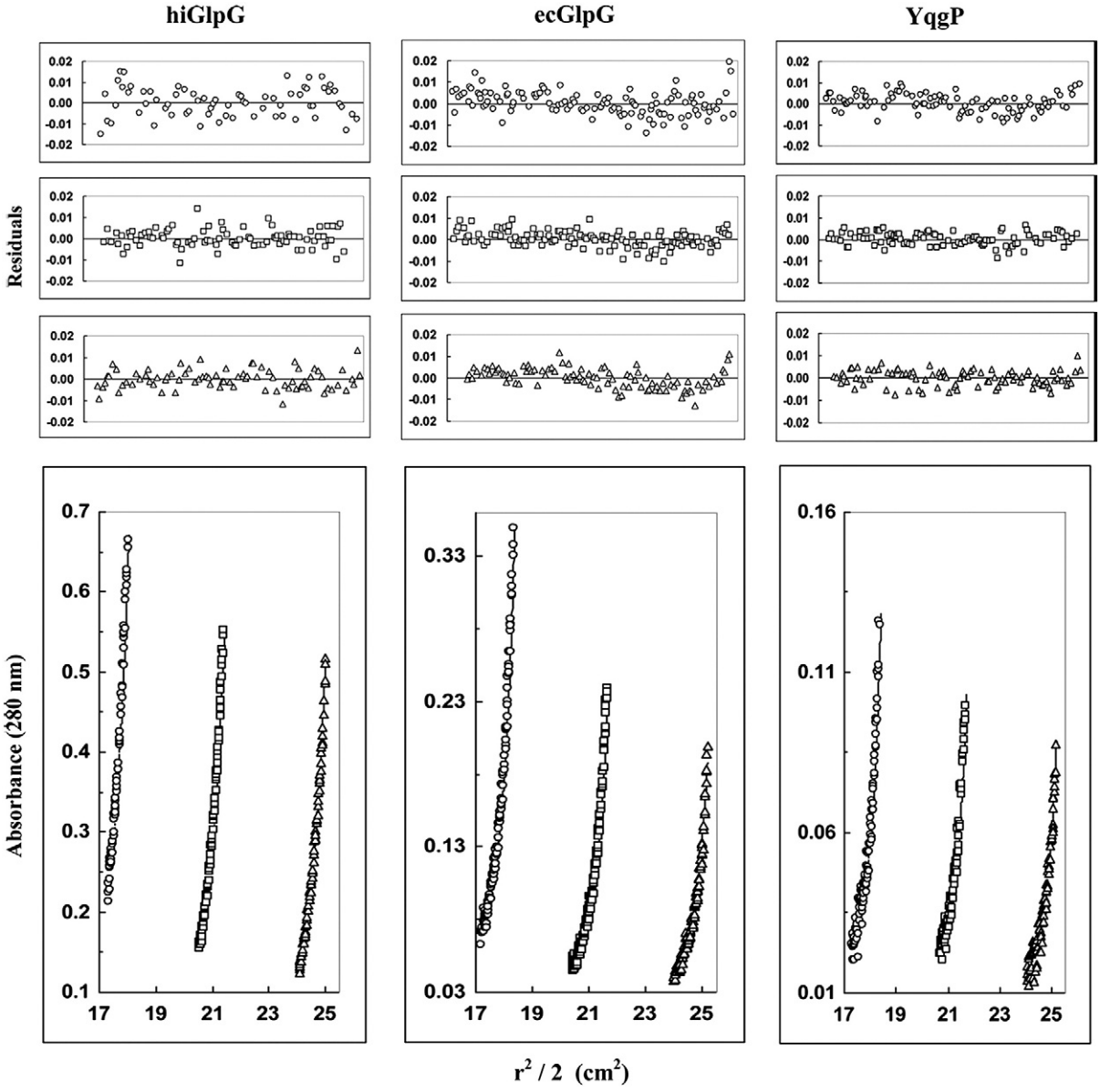

Fig. 2. Sedimentation equilibrium analysis of *hi*GlpG, *ec*GlpG and YqgP in 0.1% DDM. All three proteins were dissolved in 20 mM Tris, 20 mM NaCl pH 8.0 and 0.05% DDM and were each centrifuged at three different rotor speeds at 20 °C. Only the data collected at the lowest rotor speeds, which are 10,000, 9000 and 8000 rpm for hiGlpG, *ec*GlpG and YqgP respectively, are shown. The protein concentrations used were 0.53 (circles), 0.35 (squares) and 0.26 mg/ml (triangles) for hiGlpG; 0.17 (circles), 0.11 (squares) and 0.08 mg/ml (triangles) for *ec*GlpG; and 0.18 (circles), 0.12 (squares) and 0.09 mg/ml (triangles) for YqgP. Lower graphs illustrate $r^2/2$ versus absorbance plots; symbols represent measured data points, and solid lines represent fit lines to a monomer–dimer–tetramer model. Upper graphs illustrate the residuals from fitting the measured data points to a three-species model. The random, nonsystematic distribution of the residuals indicates a good fit of the data to the models.

treatment for the co-expression study. A small but detectable signal was noted in the mixed membrane fraction when the blot was probed with the His-Probe antibody (Fig. 5B) suggesting only a minor disruption of the dimers by the addition of the detergent. It is clear from this result that *hi*GlpG forms oligomers, most likely dimers, in the lipid bilayer.

4. Discussion

In this manuscript, we present evidence that prokaryotic rhomboids, *hi*GlpG, *ec*GlpG and YqgP, form monomers, dimers and tetramers with dimers being the predominant species. Confirming the AU results, using both crosslinking and gel filtration, we have shown that the rhomboid 6-TMD core, represented by *hi*GlpG, is dimeric and functional. A big question was whether the dimer could be observed in the membrane bilayer *in vivo* or if it was an effect of the detergent solubilization. Our pull down assay in which we co-expressed a His-tagged *hi*GlpG and a Flag-tagged *hi*GlpG demonstrates that these dimers exist *in vivo* (Fig. 5). To test if the homogenization step during purification altered the oligomers, we conducted a control where membrane fractions harboring only *hi*GlpG-His or *hi*GlpG-Flag were mixed prior to co-immunoprecipitation. This control was used to demonstrate that the detergent or the mechanical steps during purification did not disrupt or affect the native dimers found in the membrane. Only a faint signal was observed when Flag immunoprecipitations were probed with His probe suggesting a slight disruption of *hi*GlpG-Flag homodimer to form a *hi*GlpG-Flag and *hi*GlpG-His heterodimer. The co-IP experiments also suggest that the dimer is not easily separated. Unfortunately, we have not identified any conditions that disrupt the dimer and therefore cannot assess that the dimeric species is essential for function.

The rationale for the rhomboid dimerization may be two-fold: it may assist with either function and/or stability. Rhomboid peptidases

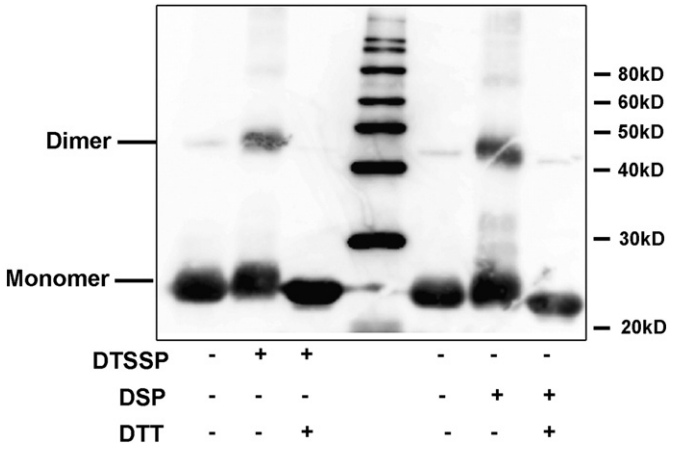

Fig. 3. Crosslinking of hiGlpG in detergent solution detected by Western blot using His-Probe. His-Probe detection of detergent solubilized *hi*GlpG 10 μg (20 μl) aliquots incubated with 1 mM DTSSP and DSP crosslinking agents, with and without the reducing agent DTT. The position of monomer and dimer are at approximately 23 kDa and 45 kDa respectively.

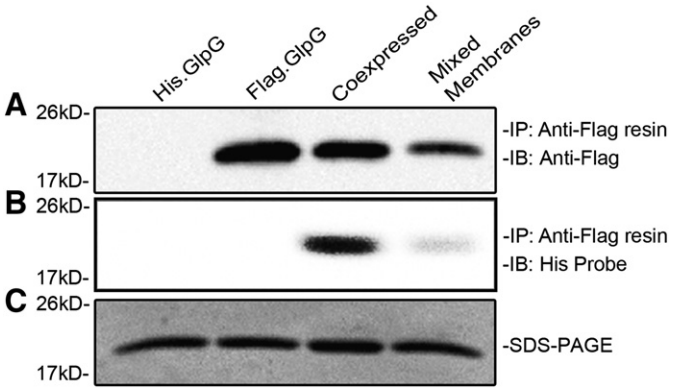

Fig. 5. Pull down assay with co-expressed His and Flag-tagged *hi*GlpG shows in vivo association. Co-immunoprecipitation assay of *hi*GlpG molecules bearing two different immunological epitopes are shown to validate the formation of *hi*GlpG dimers within the membrane bilayer. *hi*GlpG-Flag and *hi*GlpG-His were expressed either independently, or coexpressed. In addition for a control, *hi*GlpG-Flag and *hi*GlpG-His membrane fractions were mixed prior to immunoprecipitation. Upon anti-Flag immunoprecipitation, each fraction was separated on a 12% SDS-PAGE gel and analyzed by immunoblotting with either (A) anti-Flag or (B) His-Probe. (C) A Coomassie stained gel with the four different membrane fractions is shown as a loading control to ensure that equal amounts of protein were added to the resin. Molecular mass markers are reported in kDa on the left-hand side.

have a relaxed substrate specificity compared to soluble serine peptidases [49]. This means that other mechanisms must be present that regulate peptidase function. We have shown that *hi*GlpG, the simplest rhomboid with a core of 6 TM segments, [44] is dimeric. *ec*GlpG also has the six transmembrane core but also has a 9 kDa N-terminal cytosolic domain. YqgP is the largest rhomboid predicted to have 7 TM segments, plus an extra TM segment on the C-terminal region of the membrane domain. In addition, topology predictions indicate that YqgP may also have N- and C-terminal extensions. *hi*GlpG and *ec*GlpG are predicted to belong to the secretase topology classification devised by Freeman [47]. YqgP is proposed to belong to the secretase-type, 6 + 1 class of rhomboids. Given the varied topology, all three forms have in common a conserved membrane domain core that is most likely the mechanism for association. It is tempting to speculate that all members of the rhomboid family may form dimers including eukaryotic homologs.

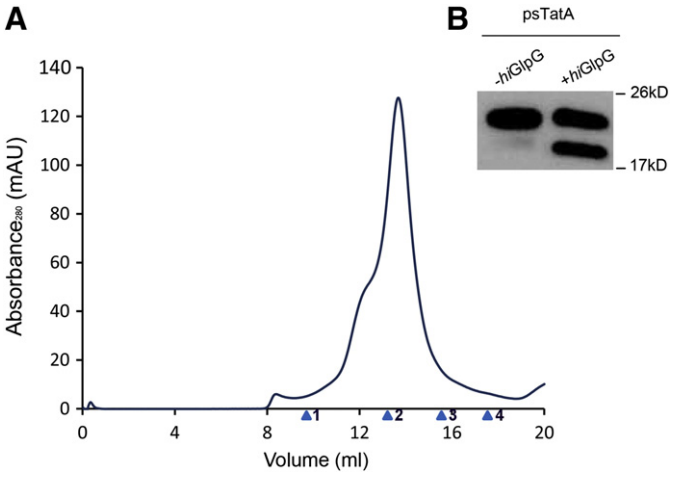

Fig. 4. Gel filtration and functional assay of *hi*GlpG. (A). Gel filtration of *hi*GlpG in 0.1% DDM. Approximately 200 μg of Ni-NTA purified *hi*GlpG in DDM was subjected to gel filtration onto a Hiload Superdex 200 10/300 column (GE Healthcare, USA) containing 50 mM Tris, 200 mM NaCl, and 5% glycerol, pH 8.0 supplemented with 0.1% DDM. Vo — void volume, Vt — total column volume 24 ml. Arrowheads represent the standard proteins from left to right: 1. thyroglobulin (MW, 670 k; Stokes radius 85 Å); 2. IgG (MW 158, stokes radius 55 Å); 3. ovalbumin; (MW 44 k; Stokes radius 30.5 Å); 4. myoglobin (MW 17 k, Stokes radius 20.7 Å); 5. (B). Rhomboid cleavage activity on *ps*TatA. SDS-PAGE demonstrating *Providencia stuartii* TatA (psTatA) substrate cleavage by *hi*GlpG in 0.1% DDM. Samples run include a control on the left panel. Molecular mass markers are reported in kDa on the left-hand side.

In our crystal structure we do not see evidence of a physiological dimer in the *H. influenza* however a crystallographic dimer with head-to-tail packing was observed [22] similar to that seen in the various *E. coli* rhomboid structures from three dimensional crystals [23–25]. Recently a projection map from 2D crystals of *ec*GlpG was presented [50]. It is clear from this map that *ec*GlpG exists as a dimer in the asymmetric unit. A three dimensional map was not presented for this data nor was the crystal structure docked into the data. Therefore it is difficult to predict where the dimer interface may lie in the protein. Since the dimer is functional, it is tempting to speculate that the conserved Loop 1 on the opposite face of the substrate entry may facilitate this dimerization. New crystal forms of *ec*GlpG membrane domain have revealed a trimer yet this packing is most likely crystallographic as the active site gating motifs, helix 5 and loop 5 (cap) are toward the center preventing easy access to the active site residues [30,31]. While we observe a band near the predicted trimer molecular weight for *hi*GlpG, it is very faint. Furthermore, we do not see a strong evidence of a physiological trimer *in vitro*, as only dimers and tetramers are observed in the gel filtration and analytical ultracentrifugation experiments.

The observation of a monomer in a crystal structure where the functional unit is dimeric in the membrane has been previous described with the sodium proton antiporter, NhaA [51]. This transporter was shown to be dimeric in two dimensional crystals [52] as well as by other biochemical methods such as crosslinking [36] and EPR [53], yet the three-dimensional crystal structure depicted a monomer [54]. It was later revealed that the dimerization was important to maintain the transporter under stress conditions during cell growth such as alkaline pH or high temperatures [55,56]. The dimerization interface was shown to occur with the β-hairpin found on the periplasmic face of the membrane boundary [53]. There are other examples of membrane proteins that oligomerize to regulate function. For the anion exchanger, AE1, the protein exists in equilibrium between dimers and tetramers. Although the monomer was thought to be the functional unit, a recent paper proposes that dimers are the functional units with each unit regulating the other allosterically [57].

The fact that rhomboids may homo-oligomerize was briefly eluded to in studies with *ec*GlpG [28]. YqgP was also found to oligomerize into large aggregates, however this study was carried out in the absence of detergent which may have facilitated oligomerization [58]. Our study explores the details of this oligomerization. There are also new questions prompted by these results. For example, does the dimerization affect the rate of substrate cleavage? Currently no proper kinetic assay

exists to address this. It is also of interest whether lipids can affect the dimerization and subsequent cleavage of substrates by rhomboid [35]. Lipids, modeled as phosphatidic acid, were found in association with the *hi*GlpG structure [22] as well as with a recent bicelle structure [50]. It is possible that the lipid environment may play a role in the oligomerization and subsequent catalytic capacity of rhomboid peptidases.

5. Conclusion

Rhomboid peptidases play key roles in many regulatory processes by cleaving substrates in their membrane environment. Elucidating the mechanism by which this cleavage takes place in this environment will be of great interest to both the membrane protein and peptidase communities. The fact that three prokaryotic rhomboid peptidases behave as oligomers suggests a common mechanism for proteolysis for this widely conserved family of membrane proteins. This paper reports the first characterization of the oligomeric state of the rhomboid family of proteins. Further study is needed to identify the interface for the dimers and whether the oligomeric state has an important role in regulating efficiency for this interesting class of intramembrane peptidases.

Supplementary data to this article can be found online at http://dx.doi.org/10.1016/j.bbamem.2012.08.004.

Acknowledgements

We thank Dr. Matthew Freeman for his kind gift of the *P. stuartii* TatA gene. We also thank all members of the Lemieux lab for their advice and reading of the manuscript. This work has been supported by the Canadian Institute for Health Research (CIHR) and Alberta Innovates Health Solutions (AIHS). Infrastructure used in this work was funded by the Canadian Foundation for Innovation. M. Joanne Lemieux acknowledges support from the Canada Research Chairs Program and the Alberta Heritage Foundation for Medical Research Scholar program.

References

[1] A.J. Barrett, N.D. Rawlings, E.A. O'Brien, The MEROPS database as a protease information system, J. Struct. Biol. 134 (2001) 95–102.
[2] J.D. Wasserman, S. Urban, M. Freeman, A family of rhomboid-like genes: *Drosophila* rhomboid-1 and roughoid/rhomboid-3 cooperate to activate EGF receptor signaling, Genes Dev. 14 (2000) 1651–1663.
[3] J.C. Pascall, K.D. Brown, Characterization of a mammalian cDNA encoding a protein with high sequence similarity to the *Drosophila* regulatory protein rhomboid, FEBS Lett. 429 (1998) 337–340.
[4] M. Freeman, Rhomboid proteases and their biological functions, Annu. Rev. Genet. 42 (2008) 191–210.
[5] S. Urban, G. Brown, M. Freeman, EGF receptor signalling protects smooth-cuticle cells from apoptosis during *Drosophila* ventral epidermis development, Development 131 (2004) 1835–1845.
[6] Z. Yan, H. Zou, F. Tian, J.R. Grandis, A.J. Mixson, P.Y. Lu, L.Y. Li, Human rhomboid family-1 gene silencing causes apoptosis or autophagy to epithelial cancer cells and inhibits xenograft tumor growth, Mol. Cancer Ther. 7 (2008) 1355–1364.
[7] H. Zou, S.M. Thomas, Z.W. Yan, J.R. Grandis, A. Vogt, L.Y. Li, Human rhomboid family-1 gene RHBDF1 participates in GPCR-mediated transactivation of EGFR growth signals in head and neck squamous cancer cells, FASEB J. 23 (2009) 425–432.
[8] M.C. Abba, E. Lacunza, M.I. Nunez, A. Colussi, M. Isla-Larrain, A. Segal-Eiras, M.V. Croce, C.M. Aldaz, Rhomboid domain containing 2 (RHBDD2): a novel cancer-related gene over-expressed in breast cancer, Biochim. Biophys. Acta 1792 (2009) 988–997.
[9] C. Adrain, K. Strisovsky, M. Zettl, L. Hu, M.K. Lemberg, M. Freeman, Mammalian EGF receptor activation by the rhomboid protease RHBDL2, EMBO Rep. 12 (2011) 421–427.
[10] C.P. Blobel, ADAMs: key components in EGFR signalling and development, Nat. Rev. Mol. Cell Biol. 6 (2005) 32–43.
[11] G.A. McQuibban, S. Saurya, M. Freeman, Mitochondrial membrane remodelling regulated by a conserved rhomboid protease, Nature 423 (2003) 537–541.
[12] R.B. Hill, L. Pellegrini, The PARL family of mitochondrial rhomboid proteases, Semin. Cell Dev. Biol. 21 (2010) 582–592.
[13] G.A. McQuibban, The PARLance of Parkinson disease, Autophagy (2011) 790–792.
[14] C. Frezza, S. Cipolat, O. Martins de Brito, M. Micaroni, G.V. Beznoussenko, T. Rudka, D. Bartoli, R.S. Polishuck, N.N. Danial, B. De Strooper, L. Scorrano, OPA1 controls apoptotic cristae remodeling independently from mitochondrial fusion, Cell 126 (2006) 177–189.
[15] I.M. Vera, W.L. Beatty, P. Sinnis, K. Kim, Plasmodium protease ROM1 is important for proper formation of the parasitophorous vacuole, PLoS Pathog. 7 (2011) e1002197.
[16] S. Urban, D. Schlieper, M. Freeman, Conservation of intramembrane proteolytic activity and substrate specificity in prokaryotic and eukaryotic rhomboids, Curr. Biol. 12 (2002) 1507–1512.
[17] P.N. Rather, X. Ding, R.R. Baca-DeLancey, S. Siddiqui, Providencia stuartii genes activated by cell-to-cell signaling and identification of a gene required for production or activity of an extracellular factor, J. Bacteriol. 181 (1999) 7185–7191.
[18] R.E. Dalbey, P. Wang, J.M. van Dijl, Membrane proteases in the bacterial protein secretion and quality control pathway, Microbiol. Mol. Biol. Rev. 76 (2012) 311–330.
[19] A. Camilli, B.L. Bassler, Bacterial small-molecule signaling pathways, Science 311 (2006) 1113–1116.
[20] L.R. Mesak, F.M. Mesak, M.K. Dahl, Expression of a novel gene, gluP, is essential for normal Bacillus subtilis cell division and contributes to glucose export, BMC Microbiol. 4 (2004) 13.
[21] K.M. Clemmer, G.M. Sturgill, A. Veenstra, P.N. Rather, Functional characterization of *Escherichia coli* GlpG and additional rhomboid proteins using an aarA mutant of *Providencia stuartii*, J. Bacteriol. 188 (2006) 3415–3419.
[22] M.J. Lemieux, S.J. Fischer, M.M. Cherney, K.S. Bateman, M.N.G. James, Rhomboid peptidase from *Haemophilus influenzae*: insights into the mechanism of intramembrane proteolysis from the crystal structure, PNAS 104 (3) (2006) 750–754.
[23] Y. Wang, Y. Zhang, Y. Ha, Crystal structure of a rhomboid family intramembrane protease, Nature 444 (2006) 179–180.
[24] Z. Wu, N. Yan, L. Feng, A. Oberstein, H. Yan, R.P. Baker, L. Gu, P.D. Jeffrey, S. Urban, Y. Shi, Structural analysis of a rhomboid family intramembrane protease reveals a gating mechanism for substrate entry, Nat. Struct. Mol. Biol. 13 (2006) 1084–1091.
[25] A. Ben-Shem, D. Fass, E. Bibi, Structural basis for intramembrane proteolysis by rhomboid serine proteases, Proc. Natl. Acad. Sci. U.S.A. 104 (2007) 462–466.
[26] K.R. Vinothkumar, Structure of rhomboid protease in a lipid environment, J. Mol. Biol. 407 (2011) 232–247.
[27] M.K. Lemberg, J. Menendez, A. Misik, M. Garcia, C.M. Koth, M. Freeman, Mechanism of intramembrane proteolysis investigated with purified rhomboid proteases, EMBO J. 24 (2005) 464–472.
[28] S. Maegawa, K. Ito, Y. Akiyama, Proteolytic action of GlpG, a rhomboid protease in the *Escherichia coli* cytoplasmic membrane, Biochemistry 44 (2005) 13543–13552.
[29] O.D. Ekici, M. Paetzel, R.E. Dalbey, Unconventional serine proteases: variations on the catalytic Ser/His/Asp triad configuration, Protein Sci. 17 (2008) 2023–2037.
[30] K.R. Vinothkumar, K. Strisovsky, A. Andreeva, Y. Christova, S. Verhelst, M. Freeman, The structural basis for catalysis and substrate specificity of a rhomboid protease, EMBO J. 29 (2011) 3797–3809.
[31] Y. Xue, S. Chowdhury, X. Liu, Y. Akiyama, J. Ellman, Y. Ha, Conformational change in rhomboid protease GlpG induced by inhibitor binding to its S′ subsites, Biochemistry 51 (2012) 3723–3731.
[32] Y. Xue, Y. Ha, Catalytic mechanism of rhomboid protease GlpG probed by 3,4-dichloroisocoumarin and diisopropyl fluorophosphonate, J. Biol. Chem. 287 (2012) 3099–3107.
[33] C.L. Brooks, C. Lazareno-Saez, J.S. Lamoureux, M.W. Mak, M.J. Lemieux, Insights into substrate gating in *H. influenzae* rhomboid, J. Mol. Biol. 407 (2011) 687–697.
[34] R.P. Baker, K. Young, L. Feng, Y. Shi, S. Urban, Enzymatic analysis of a rhomboid intramembrane protease implicates transmembrane helix 5 as the lateral substrate gate, Proc. Natl. Acad. Sci. U.S.A. 104 (2007) 8257–8262.
[35] S. Urban, M.S. Wolfe, Reconstitution of intramembrane proteolysis in vitro reveals that pure rhomboid is sufficient for catalysis and specificity, Proc. Natl. Acad. Sci. U.S.A. 102 (2005) 1883–1888.
[36] Y. Gerchman, A. Rimon, M. Venturi, E. Padan, Oligomerization of NhaA, the Na^+/H^+ antiporter of *Escherichia coli* in the membrane and its functional and structural consequences, Biochemistry 40 (2001) 3403–3412.
[37] A. Karasawa, K. Mitsui, M. Matsushita, H. Kanazawa, Intermolecular cross-linking of monomers in *Helicobacter pylori* Na^+/H^+ antiporter NhaA at the dimer interface inhibits antiporter activity, Biochem. J. 426 (2010) 99–108.
[38] J.M. Salhany, R.L. Sloan, K.S. Cordes, The carboxyl side chain of glutamate 681 interacts with a chloride binding modifier site that allosterically modulates the dimeric conformational state of band 3 (AE1). Implications for the mechanism of anion/proton cotransport, Biochemistry 42 (2003) 1589–1602.
[39] T.M. Laue, W.F. Stafford III, Modern applications of analytical ultracentrifugation, Annu. Rev. Biophys. Biomol. Struct. 28 (1999) 75–100.
[40] M.L. Johnson, J.J. Correia, D.A. Yphantis, H.R. Halvorson, Analysis of data from the analytical ultracentrifuge by nonlinear least-squares techniques, Biophys. J. 36 (1981) 575–588.
[41] T.M. Laue, B.D. Shah, T.M. Ridgeway, S.L. Pelletier, Analytical Ultracentrifugation in Biochemistry and Polymer Science, R. Soc. Chem, Cambridge, UK, 1991.
[42] F. Reiss-Husson, Crystallization of Membrane Proteins, IRL Press, Oxford, 1991.
[43] T.C. Laurent, J. Killander, A theory of gel filtration and its experimental verification, J. Chromatogr. 14 (1964) 303–316.
[44] M.J. Lemieux, S.J. Fischer, M.M. Cherney, K.S. Bateman, M.N. James, The crystal structure of the rhomboid peptidase from *Haemophilus influenzae* provides insight into intramembrane proteolysis, Proc. Natl. Acad. Sci. U.S.A. 104 (2007) 750–754.
[45] M.J. Lemieux, J. Song, M.J. Kim, Y. Huang, A. Villa, M. Auer, X.D. Li, D.N. Wang, Three-dimensional crystallization of the *Escherichia coli* glycerol-3-phosphate transporter: a member of the major facilitator superfamily, Protein Sci. 12 (2003) 2748–2756.
[46] R.H. Friesen, J. Knol, B. Poolman, Quaternary structure of the lactose transport protein of *Streptococcus thermophilus* in the detergent-solubilized and membrane-reconstituted state, J. Biol. Chem. 275 (2000) 33527–33535.
[47] M.K. Lemberg, M. Freeman, Functional and evolutionary implications of enhanced genomic analysis of rhomboid intramembrane proteases, Genome Res. 17 (2007) 1634–1646.

[48] M. Auer, M.J. Kim, M.J. Lemieux, A. Villa, J. Song, X.D. Li, D.N. Wang, High-yield expression and functional analysis of *Escherichia coli* glycerol-3-phosphate transporter, Biochemistry 40 (2001) 6628–6635.
[49] K. Strisovsky, H.J. Sharpe, M. Freeman, Sequence-specific intramembrane proteolysis: identification of a recognition motif in rhomboid substrates, Mol. Cell 36 (2009) 1048–1059.
[50] K.R. Vinothkumar, Structure of rhomboid protease in a lipid environment, J. Mol. Biol. 407 (2011) 232–247.
[51] E. Padan, L. Kozachkov, K. Herz, A. Rimon, NhaA crystal structure: functional-structural insights, J. Exp. Biol. 212 (2009) 1593–1603.
[52] K.A. Williams, Three-dimensional structure of the ion-coupled transport protein NhaA, Nature 403 (2000) 112–115.
[53] D. Hilger, H. Jung, E. Padan, C. Wegener, K.P. Vogel, H.J. Steinhoff, G. Jeschke, Assessing oligomerization of membrane proteins by four-pulse DEER: pH-dependent dimerization of NhaA Na^+/H^+ antiporter of *E. coli*, Biophys. J. 89 (2005) 1328–1338.
[54] C. Hunte, E. Screpanti, M. Venturi, A. Rimon, E. Padan, H. Michel, Structure of a Na^+/H^+ antiporter and insights into mechanism of action and regulation by pH, Nature 435 (2005) 1197–1202.
[55] A. Rimon, T. Tzubery, E. Padan, Monomers of the NhaA Na^+/H^+ antiporter of Escherichia coli are fully functional yet dimers are beneficial under extreme stress conditions at alkaline pH in the presence of Na^+ or Li^+, J. Biol. Chem. 282 (2007) 26810–26821.
[56] K. Herz, A. Rimon, G. Jeschke, E. Padan, Beta-sheet-dependent dimerization is essential for the stability of NhaA Na^+/H^+ antiporter, J. Biol. Chem. 284 (2009) 6337–6347.
[57] J.M. Salhany, Stilbenedisulfonate binding kinetics to band 3 (AE 1): relationship between transport and stilbenedisulfonate binding sites and role of subunit interactions in transport, Blood Cells Mol. Dis. 27 (2001) 127–134.
[58] X. Lei, K. Ahn, L. Zhu, I. Ubarretxena-Belandia, Y.M. Li, Soluble oligomers of the intramembrane serine protease YqgP are catalytically active in the absence of detergents, Biochemistry 47 (2008) 11920–11929.